Identification and Measurement of Biomarkers at Single Microorganism Level for In Situ Monitoring Deep Ultraviolet Disinfection Process

Yuxuan Xue[1], Ye Ma[1], Zhiyong Sun[2], Xinyu Liu[1], Mukun Zhang[1], Jiawei Zhang[3], Ning Xi[1]

***Abstract*—Since the COVID-19 disease has been further aggravated, the prevention of pathogen transmission becomes a vital issue to restrain casualties. Recent research outcomes have shown the possibilities of the viruses existing on inanimate surfaces up to few days, which carry the risk of touch propagation of the disease. Deep ultraviolet germicide irradiation (UVGI) with the wavelength of 255–280nm has been verified to efficiently disinfect various types of bacteria and virus, which could prevent the aggravation of pandemic spread. Even though considerable experiments and approaches have been applied to evaluate the disinfection effects, there are only few reports about how the individual bio-organism behaves after ultraviolet C (UVC) irradiation, especially in the aspect of mechanical changes. Furthermore, since the standard pathway of virus transmission and reproduction requires the host cell to assemble and transport newly generated virus, the dynamic response of infectious cell is always the vital aspect of virology study. In this work, high power LEDs array has been established with 270nm UVC irradiation to evaluate disinfection capability on various types of bio-organism, and incubator embedded atomic force microscopy (AFM) is used to investigate the single bacterium and virus under UVGI. The real-time tracking of the living Vero cells infected with adenovirus has also been presented in this study. The results show that after sufficient UVGI, the outer shell of bacteria and viruses remain intact in structure, however the bio-organisms lost the capability of reproduction and normal metabolism. The experiment results also indicate that once the host cell is infected with adenovirus, the rapid production of newborn virus capsid will gradually destroy the cellular normal metabolism and lose mechanical integrity.**

***Index Terms*—atomic force microscopy, deep ultraviolet irradiation, living cell, adenovirus, mechanical properties**

I. Introduction

The outbreak of the 2019 coronavirus (COVID-19) has been regarded as a public health emergency of international concern and infected over millions of people. These numbers are continually increasing and the severe situation has caused global panic[1]. In general, besides respiratory droplets, fomites, physical touches are also the critical transmission approach of coronaviruses. That said, current evidence suggests that coronavirus can remain viable on many surfaces for several days, especially when Omicron has more stability compared with the parental viruses[2]–[4]. Even though infection prevention approaches such as chemical reagent have the significant effects on killing the bacteria and viruses[5],

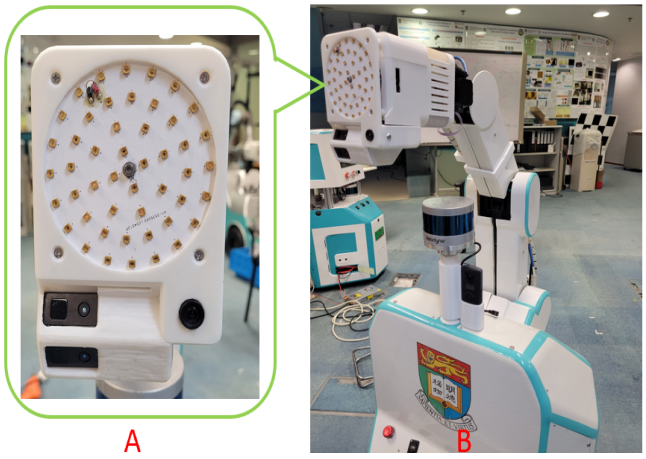

Fig. 1. (A): Setup of the 270nm UVC irradiation LEDs array with 48 individual LED. (B): UVC LEDs array carried by home-designed autonomous robot.

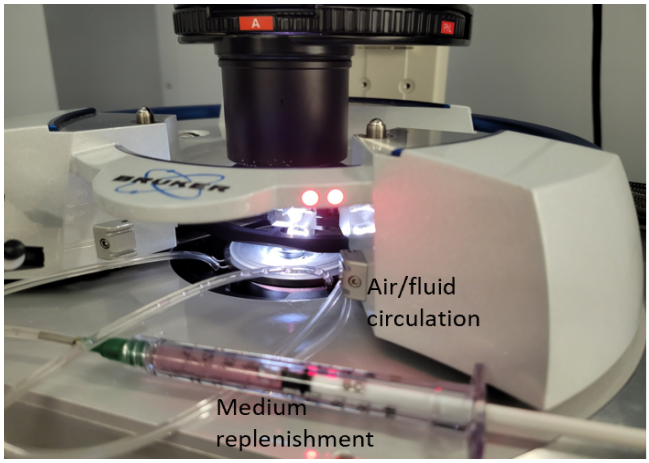

Fig. 2. AFM system with air/fluid circulation incubator for measurement whilst the cells remain alive.

The work described in this paper was partially supported by a grant from RGC General Research Fund (17209521), Electrical and Mechanical Services Department, the Innovation and Technology Commission of the Hong Kong Special Administrative Region, China (SST/121/20GP),Basic Research Program of Shenzhen (JCYJ20170818105718495, and JCYJ20180504170303184) and the National Natural Science Foundation of China (Grant Nos. 61727811, U1813214, and U1813210)(Corresponding authors: N. Xi, J. Zhang, Z.Sun).

[1]Yuxuan Xue, Ye Ma, Xinyu Liu, Mukun Zhang, and Ning Xi are with the Department of Industrial and Manufacturing Systems Engineering, The University of Hong Kong,Pokfulam, Hong Kong (e-mail: xueyuxuan@hku.hk;xining@hku.hk).

[2]Zhiyong Sun is with the Institute of Intelligent Machines, Hefei Institute of Physical Science, CAS, Hefei, 230031, China. (e-mail: sunzy@iim.ac.cn).

[3]Jiawei Zhang is with Shenzhen Academy of Robotics, Shenzhen, Guangdong 518000, China (e-mail: 353302105@qq.com).

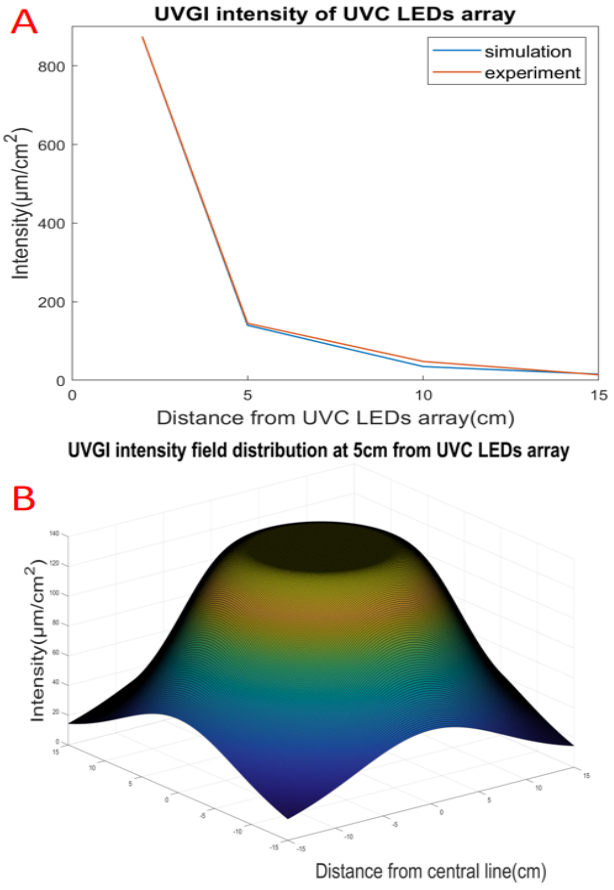

Fig. 3. (A): UVGI intensity of UVC LEDs array along the central line from the LED center. (B): Simulated UVGI intensity field distribution at 5cm from UVC LEDs array.

[6]. they are causing inconvenience such as residue and damaging public disinfection procedures, therefore further improvements are necessary. Ultraviolet (UV) light-emitting diodes (LEDs) are an emerging technology for antivirus and antibacterial disinfection[7]. Considerable research into UVC irradiation with 255–285nm has been tested on inactivating in bacteria, viruses, and other contaminates. Short-wavelength ultraviolet or UVC irradiation has been tested on inactivating bacteria, viruses, and other contaminates[8].UVGI has the ability to inactivate microorganisms by destroying nucleic acid genomes, leaving them unable to perform vital cellular functions with high effectiveness[9]–[11].The standard pathway of virus transmission and reproduction requires the virus shell to disassemble and transport the viral genome into the host cell. Virus infection of eukaryotic cells typically requires four steps: attachment; disassembly; release of viral genome into the host cell that replicates the viral gene and package new virus; and finally egression and location of the next target cell[12], [13]. The dynamic response of cellular behavior in the aspects of morphology and mechanical properties under virus attack is essential for clinical development, where the adoption of deep UVGI especially around 270nm could destroy the viral infectivity which can be revealed by the infectious status of host cells[14].There are types of approaches to evaluate the effectiveness of virus and bacteria disinfection, such as carrier, in-use and field test with the culture and molecular based analysis methods for bacteria disinfection evaluation[15];immunofluorescence and Elisa methods for virus disinfection evaluation[16], [17]. These methods could evaluate the disinfection effects based on the behavior of colonial of bio-organism, however they heavily rely on the statistical data and require time to acquire the results. Furthermore, how the single bio-organism changes during the disinfection procedure is hard to track with these approaches. Mechanical biomarkers such as elasticity and viscosity are heavily connected to the status of proteins and DNA in single microorganism[18]. The protein especially cytoskeletal protein such as MreB and FtsZ in bacteria regulate and construct the mechanical structure of the microorganism[19]. The DNA structures and properties control the activities like replication, transcription and super-coiling then affect the biological functions of the single microorganism including mechanical behavior[20], [21]. However, there is lack of evidence for the UVGI disinfection effects for morphological and mechanical change in single microorganism which is regulated by the status of DNA and protein. To evaluate the mechanical change in a single microorganism level, especially under the native growing environment, the atomic force microscopy (AFM) has been adopted to improve the evaluation procedure for UVGI disinfection effects.

AFM is one of the most powerful research platforms to study the morphology of living bio-organism whilst measuring the object's mechanical properties simultaneously[22]–[24]. In AFM, the force actuator drives the probe with a very tiny tip located near the top of cantilever. While scanning, the deflection of the cantilever is received by the position sensitive device (PSD). The topography image of the sample is obtained by modeling the deflection cantilever and the scanner's initial position. This mechanical interaction enables the system for characterizing the structures and properties of living biological systems in their native states under aqueous conditions with unprecedented spatial resolution[25].The importance of mechanobiology of single cells has been comprehensively researched by AFM to record the changes of cell profiles correlated with changes in cellular states, fate decisions, and disease progression[26], [27].There are also research in virology that investigated the mechanical fatigue of virus shell under the external force, chemical reagent and other external disturbance by real-time measurement of AFM [28], [29].

In this work, for the reason of systemically understanding the mechanism of bio-organism behavior under the irradiation of deep UV light, to start, we designed the high power UVC LED array that was carried out by the autonomous robot which is detailed elsewhere[30]. Under the UVC irradiation situation, the virus ability of invading cell and proliferation of bacteria have been researched. The experiments with UVGI increment have been designed, the survival rate of the Escherichia Coli (E.coli) and adenovirus decreases with the dosage of 270nm UVGI. Our findings also show that the outer capsid of adenovirus and the shell of E.coli still remain intact after high dosage of deep UVGI. To further understand the UVC disruption effect on the bioorganisms within the single cell

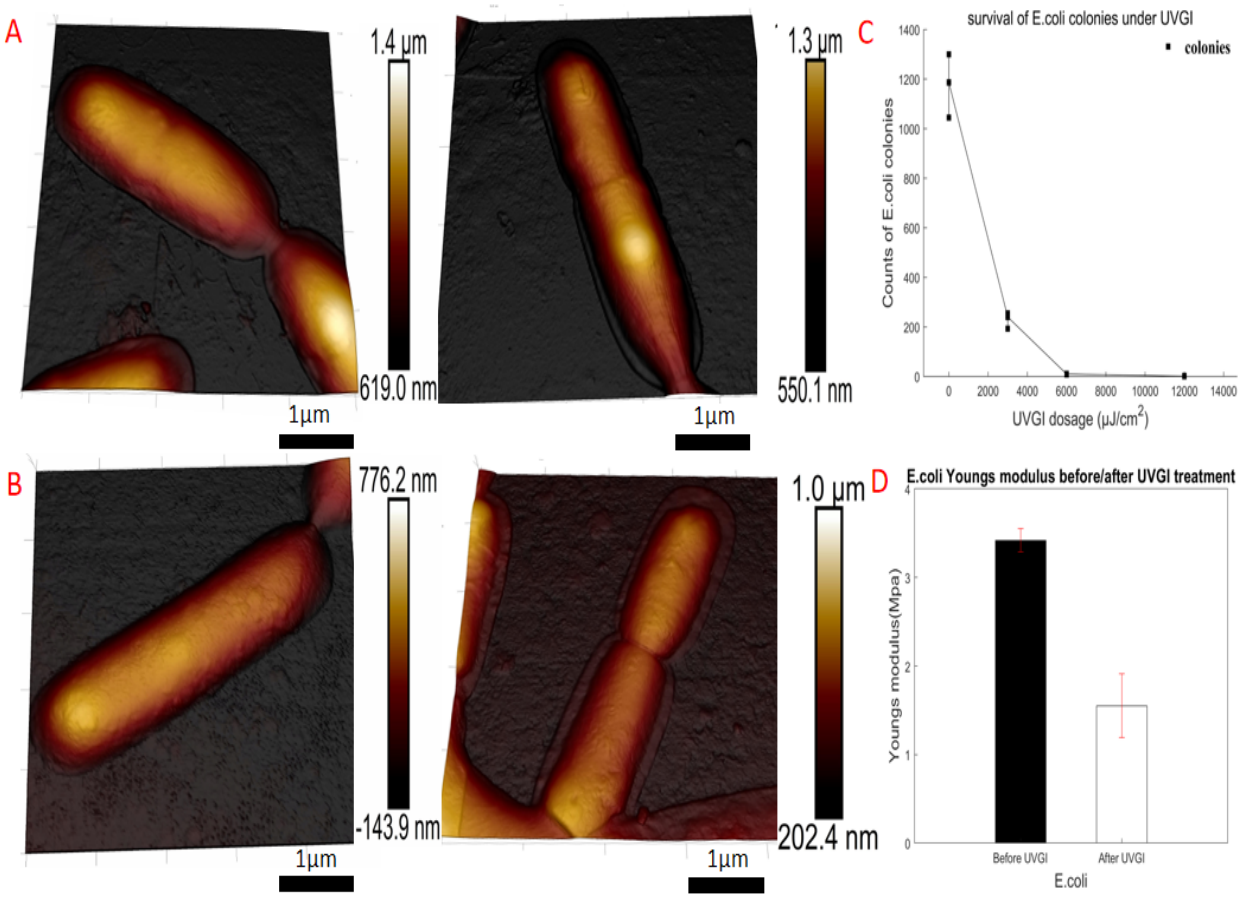

Fig. 4. (A): AFM topography of E.coli grow on LB medium without UVGI treatment. Scale bar: 1µm. (B): AFM topography of E.coli with UVGI treatment. Scale bar: 1µm. (C): E.coli survival curves of proliferation colonials by 270nm UVGI.(D): The Young's Modulus distribution of E.coli before and after 20mj/cm^2 irradiation : 3.42±0.13Mpa and 1.55±0.36Mpa. (Biological Repeat N$>$ 3; 256 curves per cell; p$<$0.001).

level, the cell incubator system with air/fluid circulation and medium replenishment has been embedded to AFM to track the real-time change of single cell morphology and mechanical response under infectious and disinfected condition[31]. The single-cell tracking during the time lapse would collect time-dependent morphology and mechanical response with the virus invading the production cycle, which could further verify the UVC disinfection effects and cellular behavior change under the infectious.

II. Material and Method

A. Biological samples preparation

Rod-shaped bacterium E.coli. (ATCC 25922) and GRF transfected adenovirus (PAV[exp]-cmv$>$EGFP) 25ul per vial were prepared for the study (Vector Builder, Inc). Bacteria were cultured overnight in Luria-Bertani medium (Sigma-Aldrich, Inc) and tryptic soy agar (Liofilch, Inc) substrate for the proliferation and AFM measurement respectively. The Vero E6 kidney epithelial cells were acquired from the ECACC and cultured in DMEM supplemented with 10% FBS, and 1% penicillin-streptomycin (Sigma-Aldrich, Inc) under the $37°C$ and 5% CO2 in the incubator for regular cultivation. For the AFM incubated measurement, an additional 10mM HEPES (Sigma-Aldrich, Inc) was added to the cultural medium to maintain the pH level. Before the AFM measurement, one part of the E.coli had been directly derived from the culture medium and located on the petri dish for the UVC irradiation, and the other part of E.coli was centrifuged with 2000g for 15 minutes for the purpose of getting rid of impurity. The cleaved mica was first merged into 10% APTES (Sigma-Aldrich, Inc) for 1 hour to create an amino surface, washed with DI water thoroughly, then a 20µl virus solution was coated on the mica for 15 minutes, after coating, the sample was washed with DI water three times and dried before measurement.

B. UVC LEDs disinfection efficiency with bacteria proliferation test

The tryptic Soy Agar (TSA) test for the growth of bacteria was adopted to measure the disinfection effects of 270nm UVGI to E.coli. With the bacteria cultured in LB medium, the bacteria solution has been located at the distance of UVGI irradiation of 100W/cm^2, the groups (at least 3 biological repeats for each condition) of bacteria were treated with UVC irradiation with time of 0s, 30s, 60s and 90s respectively. After the UVGI treatment, the TSA plates were replaced to the incubator 24 hours. After incubation, the colonial data were photographed and counted accordingly.

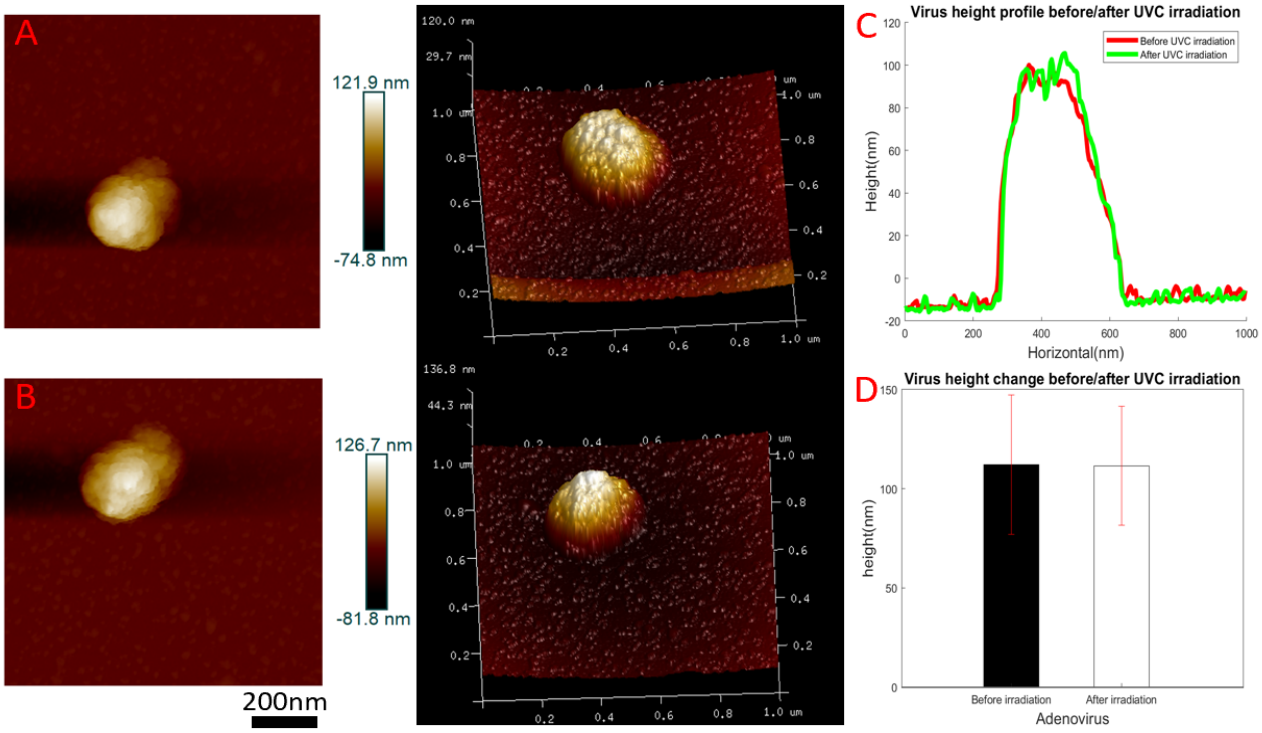

Fig. 5. High resolution topography of adenovirus: (A): adenovirus before irradiation 2D: left; 3D: right. Scale bar: 200nm.(B): adenovirus after 100 radiation 2D: left 3D: right. Scale bar: 200nm. (C): Height profile of adenovirus before and after 100mj/cm^2 UVC irradiation along the apex of adenovirus. (D): Height statistics of adenovirus: before: 112.14nm±35.22nm, N=57; after: 111.54nm ±29.94nm, N= 32.

C. Deep ultraviolet LEDs and inverse square law

The UVC LED array contained 48 individual LEDs was designed with the peak wavelength of 270nm UVC irradiation (Fig.1). The UVC LEDs array has around 3560 μW/cm^2 irradiation intensity at 1cm. According to the inverse square law, the intensity proportional to the inverse square of the distance between light source and projection location. The modified intensity distribution of UVC LEDs array segmented in two parts: the central projection area and peripheral projection area. The intensity within the central projection area remains similar and the intensity in peripheral projection decay with the distance from the central projection area, the mathematics expression is:

$$I_{UVGI} = \begin{cases} \frac{I_0 h_0^2}{h_x^2}, & s.t. 0 < r < L_0 \\ \frac{I_0 h_0^2}{h_x^2 + (r - L_0)^2}, & s.t. L_0 < r < L_{edge} \end{cases} \quad (1)$$

where h_0,I_0 is the distance and intensity at near field testing location while x is the vertical distance from projection to LEDs array. L_0 is the LEDs array width, L_{edge} is the maximum irradiation width depending on the illumination angles of UVC LED, and r is the distance from measurement point to the central line of UVC irradiation field.The dosage of bio-organism received is equal to the integral of intensity and time:

$$D = \int_0^t I_{UVGI} dt, \quad (2)$$

The intensity of 270nm UVC irradiation was measured by the UVC meter (Lin Shang, Inc) with the recording wavelength range of 220–280nm.

D. Virus infected Vero E6 cell

During the cell preparation, after the cell confluence had reached 80%, Vero E6 cells were seeded in a 96-well plate, and pillar was cloned in the petridish with the growth medium, the cells were cultivated in incubator overnight. After 24 hours, the culture medium was removed and adenovirus with the tier of 10e9/ml which was diluted in DMEM was injected into the cell culture. For UVGI disinfected groups, before injecting the virus solution to the cell dish, the virus was disinfected UVC LED to the desired dosage. The sample distance from UVC LED was controlled with the intensity of 100μw/cm^2 and the dosage equaled to the irradiation intensity multiply times . Each experiment had at least three biological repeats. After the virus injection, the well plate was cross-shaken and incubated for 8 hours, then the virus medium was removed and re-injected with culture medium. The optical images and fluorescence images were measured after the starvation procedure. Nikon Eclipse Ti-U with the black and white camera DS-Qi2 (Nikon) was used to acquire the fluorescence and optical images.

E. High resolution AFM image on incubated living cell and bio-organism

AFM images and force–distance curves were performed and recorded in culture medium using a Resolve BioAFM (Bruker). The established incubator system with air/fluid circulation, medium replenishment and heat panel were embedded

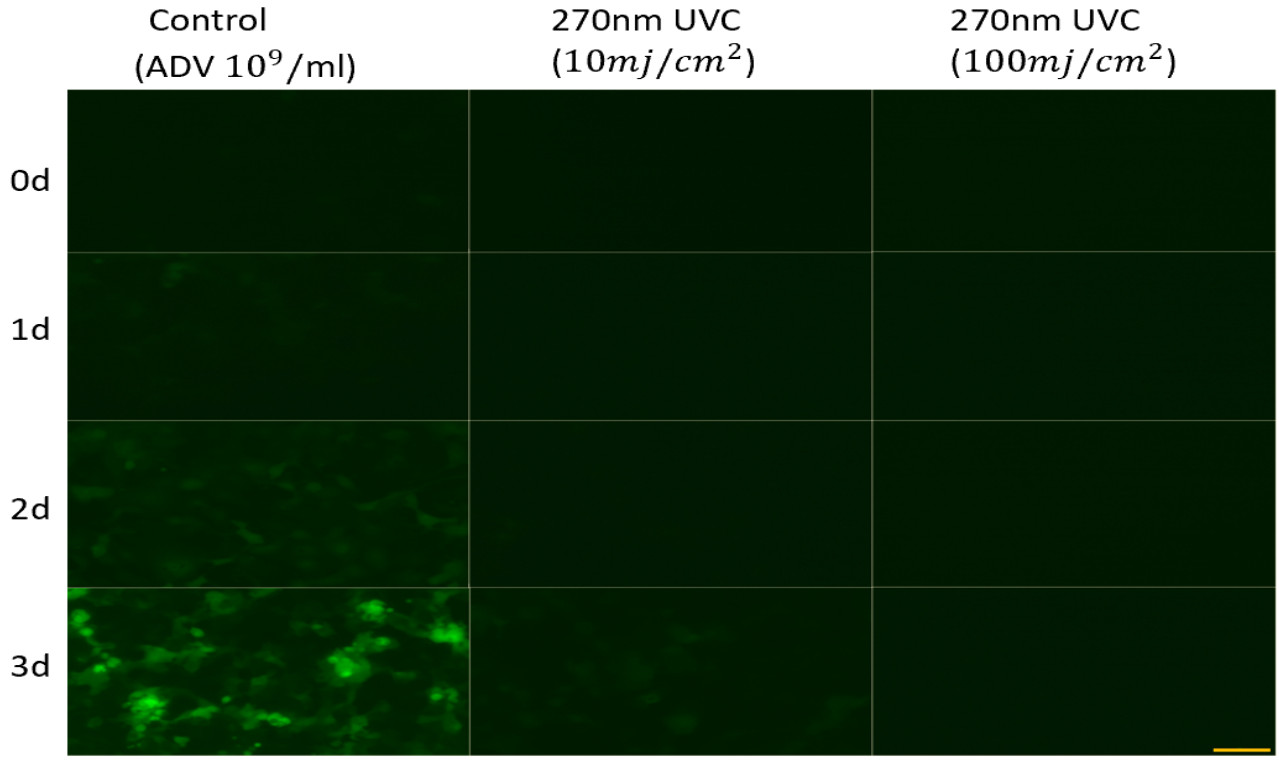

Fig. 6. Fluorescence images for adenovirus infected Vero E6 cells: left: control group; middle: infected with adenovirus concentration of 10^9/ml for 3d; right: Infected with 270nm UVC disinfected adenovirus with 100mj/cm^2 dosage concentration of 10^9/ml for 3d. 20X objective lens. Scale bar: 50μm.

with the AFM system (Fig.2). In the measurement, 3–4ml culture medium contained 10mM HEPES were gently injected to the petri dish to maintain the cell culture in the suitable liquid environment and ensure the medium emerging the whole probe to avoid the disturbance of laser light. During the measurements, the cells were growing on the incubator embedded with the AFM system. Imaging was performed in Peakforce tapping mode with PKFQNM-LC-A probes (Bruker) with the spring constant of 0.08N/m to 0.11N/m with small cantilever. The images were recorded at a scan rate of 0.3Hz, an applied force of 200–500pN, and the peakforce tapping frequency of 0.5khz to 1Khz with the resolution of 256X256 pixels. Scanning location have been selected with the image area varying from 30μmX30μm to 50μmX50μm. For the imaging of adenovirus, PEAKFORCE-HIRS-F-A probe (Bruker) with a stiffness around 0.35N/m has been selected. A very gently force was applied to image the virus, the applied force was around 30–100pN and the scan region was 1μmX1μm.

F. Force volume and mechanical properties

For each cell, a map of 16 × 16 curves was recorded on a 2μm X 2μm area on top of the cell membrane to minimize the disturbance of measurement. For mechanical analysis, since the conical tip (opening angle of 15°) has been used,the approach part of force curves was fitted with the Sneddon model to calculate the cellular Young's modulus:

$$F = \frac{2}{\pi}\frac{E}{1-\nu^2}tan(\alpha)\delta^2 \tag{3}$$

where ν is the poisson ratio of cell with the typical value of 0.5, α is the half-opening angle of the conical tip. F is the interacted force generated on AFM probe equals to the deflection of the cantilever times spring constant.Indentation depth equals to the z movement of piezo actuator subtract the deflection of cantilever.

G. Data analysis

The surface topography was analysed by the offline software Nanoscope Analysis(Bruker, Inc). The force curves and mechanical properties calculation were analyzed offline using the Nanoscope Analysis data processing software (Bruker, Inc), Matlab R2020a (Mathworks, Inc),and open source software AtomicJ[32].

III. Results

A. Deep ultraviolet irradiation prevent the proliferation of bacteria

The propagation of the UVGI obeys the inverse square law, and the intensity change of UVC irradiation is proportion to the inverse square distance from measurement point to the light source (Fig3.A,B).To verify the effectiveness of 270 nm UVC disinfection effect, the bacteria experiments have been established both in proliferation measurement and individual investigation.The results showed that the TSA test with the dosage of 0; 3000; 6000; 12000μj/cm^2 of 270nm UVGI, the average counts of the E.coli colonies for the corresponding dosage is: 1177.3; 229.3; 9.67, and 1.33, respectively. The disinfect ratio was over 99% when the dosage reached

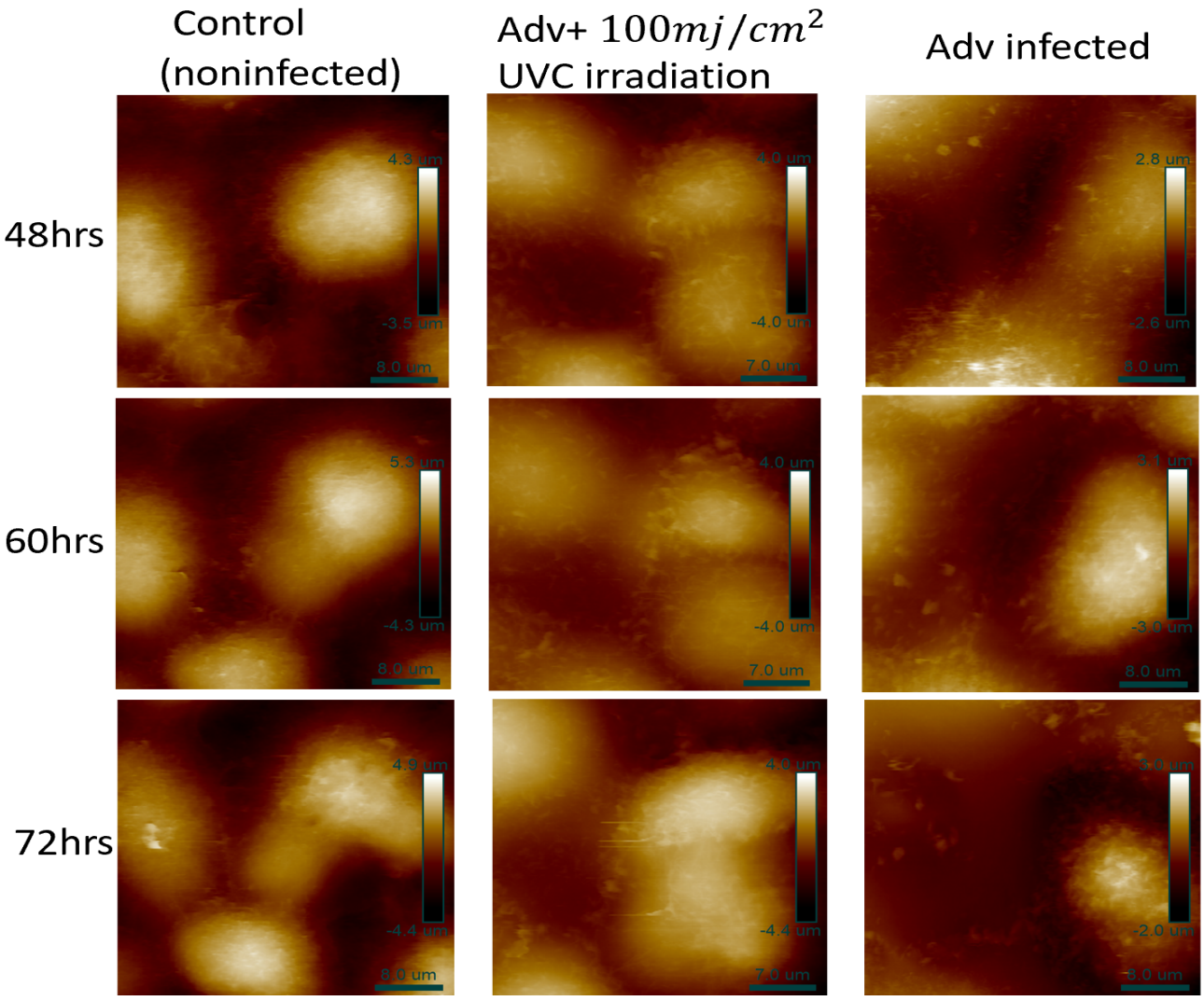

Fig. 7. High resolution AFM image for living Vero E6 cells from 48-72hrs after starvation process, left to right: control(non-infected); adenovirus injection with 100mj/cm^2 UVGI treatment,; adenovirus injection. Bottom-right scale bar: width; right scale bar: height.

12000μj/cm^2 for the E.coli (Fig.4C). The high resolution AFM topography measured E.coli morphology without destroying their native living environment (Fig.4A). The morphology of the bacteria still remained similar before and after the high dosage UVC irradiation (Fig.4B). However the mechanical properties of the bacteria were decreased may cause by the disruption of the DNA strands or functional protein groups. The indentation experiments for the E.coli were performed on the central top of bacteria with a region of 500nmX500nm. The Young's Modulus distribution of E.coli before and after 20mj/cm^2 irradiation were 3.42±0.13MPa and 1.55±0.36MPa respectively (Fig.4D) (with at least three biological repeats and over 1,000 force curves).

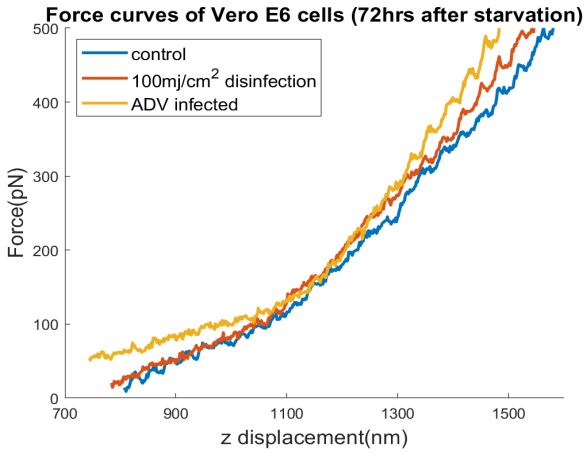

Fig. 8. AFM force curves for Vero E6 cells with 72hours incubation after starvation.

B. Deep UVGI disinfected the infectivity of virus without destroying the protein shell integrity

To assess the deep UV effect on the virus, the adenovirus samples were coated on the amino-treated mica as illustrated in the Methods part. The adenovirus was designed with two groups: one was the control group, the other was treated with 100mj/cm^2 270nm UVC irradiation. High-resolution 2D/3D topography of adenovirus before and after irradiation were

measured (Fig5A,B), the topography showed the adenovirus had the typical height from 80nm to 130nm with a round shape where the width of virus is larger than the height because of the tip convolution effect (Fig.5C). The 2D and 3D images of adenovirus capsid showed that the protein shell was constituted of protein with hexon and penton shapes[33]. Height statistics of adenovirus without irradiation was 112.14nm±35.22nm with 57 individuals count while the height after 100mj/cm^2 irradiation was 111.54nm ±29.94nm with 32 count (Fig.5D). The fluorescence results of adenovirus-infected cells with the protocol discussed above indicate the disinfection effect with 270nm UVC irradiation. The measurement was started from the procedure of starvation of adenovirus (8 hours) for Vero E6 cells and recorded every 24 hours: 0d, 1d, 2d, 3d four groups have been measured . Three experimental groups were established: starvation with DMEM medium without virus injection; 10^9PFU/ml adenovirus with 10mj/cm^2 dosage of UVGI injection;10^9PFU/ml adenovirus with 100mj/cm^2 dosage of UVGI injection. The fluorescence results showed the Vero E6 cells gradually reproduce the adenovirus with the results of green fluorescence label intensifying: with the 100mj/cm^2 270nm UVGI the virus totally lost the ability of infecting cells (Fig.6).

C. Time-dependent morphological and mechanical change of Vero cells under virus infection and deep UVGI disinfection

To further realize the infectivity and toxicity of viruses by infecting the host Vero E6 cell with/without the UVGI treatment, the group with the untreated adenoviruses injection, the group with the injection of sufficient UVGI treatment ($100mj/cm^2$) adenoviruses and negative control group has been designed. The DNA destroyed adenoviruses may still infect the host cells but lack of the ability for the complete viral replication cycle and producing new virus particles. But there may still the chance for the host to perform innate immune response which may affect the morphology and mechanical properties of the host cells[34], [35]. High-resolution AFM image for living Vero E6 cells infected by the adenovirus have performed under strict protocol with an established incubator system, and the cell membrane topography and the morphology changed accordingly for the control group, the groups infected with the adenovirus, and 100mj/cm^2 UVGI infected adenovirus with wavelength of 270nm. To monitor the whole cellular morphology details, the scan size was set as 30 μmX30μm to 50μmX50μm to ensure the whole cell body could be scanned properly, the size of the Vero cell typically has the width of 15 to 30 μm in the horizontal axis and 2 to 4 micrometers in height on the nucleus region for a normal cell. According to the high-resolution AFM images, after the adenovirus infection, compared with the control group, the cells became less adhere to the substrate and rounding. The cell-to-cell junctions gradually disappeared with the time and finally, via the cell apoptosis, no longer adhered to the substrate which cannot be measured by AFM. The topography also indicated that for the group of cells injected with UVGI-disinfected adenovirus, the membrane and morphology of cells were similar to those in the control group with minor change besides migration and proliferation (Fig.7).

D. Stiffness response for the adenovirus infected Vero cell

After the imaging of the cell topography, the mechanical properties for the cells were performed on the central top of the cell membrane with a 2μmX2μm region for multiple indentation experiments with force volume mode. In this study, the three groups of cells underwent indention experiments every 12 hours and the force curves were collected for each indentation (Fig.8). The Young's Modulus distributions of cells on the central location for the different groupscontrol; 100 UVC irradiation adenovirus infection; adenovirus injection from 48 hours to 72 hours after virus starvation: control: 10.94±4.96kPa, 12.53±6.77kPa, 11.10±5.61kPa; UVC disinfection: 13.46±4.54kPa, 11.20±3.80kPa, 12.88±6.74kPa; adenovirus: 16.40±4.68kPa, 22.03±8.24kPa, 27.79±16.47kPa (Fig.9). The results indicate the Vero cells with control and UVGI-disinfected virus injection condition had very small Young's modulus change during the incubation while for the adenovirus-infected cells, the Young's modulus increased dramatically with the time lapse. Each group had at least three biological experiment repeats and over 256 force curves for each cell were recorded (Fig.10).

IV. Discussion

Since UVC has been verified to disinfect various kinds of bio-organism, but how virus or bacteria morphology and mechanisms change still lack study. In this work, we first set up a more traditional approach to evaluate the effects of 270nm UVGI. The virus fluorescence and E.coli colonials results indicate the effectiveness of UVC LEDs, especially with the high power array we designed which could reach over 1000μw/cm^2 at a short distance. It could disinfect 99% E.coli in less than 20s, the designed LEDs could then swiftly disinfect viruses and bacteria vulnerable to UVC irradiation such as SARS-CoV-2[36]. However, as discussed above, the individual changes of bio-organisms lack investigation. Using AFM to measure the change of bio-organism in single cell level has great significance to understanding how the virus and bacteria change with irradiation. Results showed that the morphology of the bacteria and viruses still remain similar before and after the high dosage UVC irradiation. Compared with the results of fluorescence and TSA test, it is concluded that UVC damage to the protein shell's integrity was minor but could effectively eliminate the infectivity of bioorganisms. The results also indicate the stiffness of the bacteria have been changed which may cause by the disruption of the DNA stranded structures or the destroyed of specific surface protein[37].

The incubated system integrated with AFM offers a platform to realize single-cell behavior measurement through-out time with high-resolution pictures and mechanical characteristics. The findings show that adenovirus infection causes gradual changes in the morphology and stiffness distributions in Vero cells, which disturbs the normal process of cellular growth and metabolism and has an impact on the cytoskeleton structure, including F-actin and microtubules (Fig.7,Fig.9). The adenovirus entry to the cell will slowly destroy the cellular metabolism which lasts few days. The cell membrane

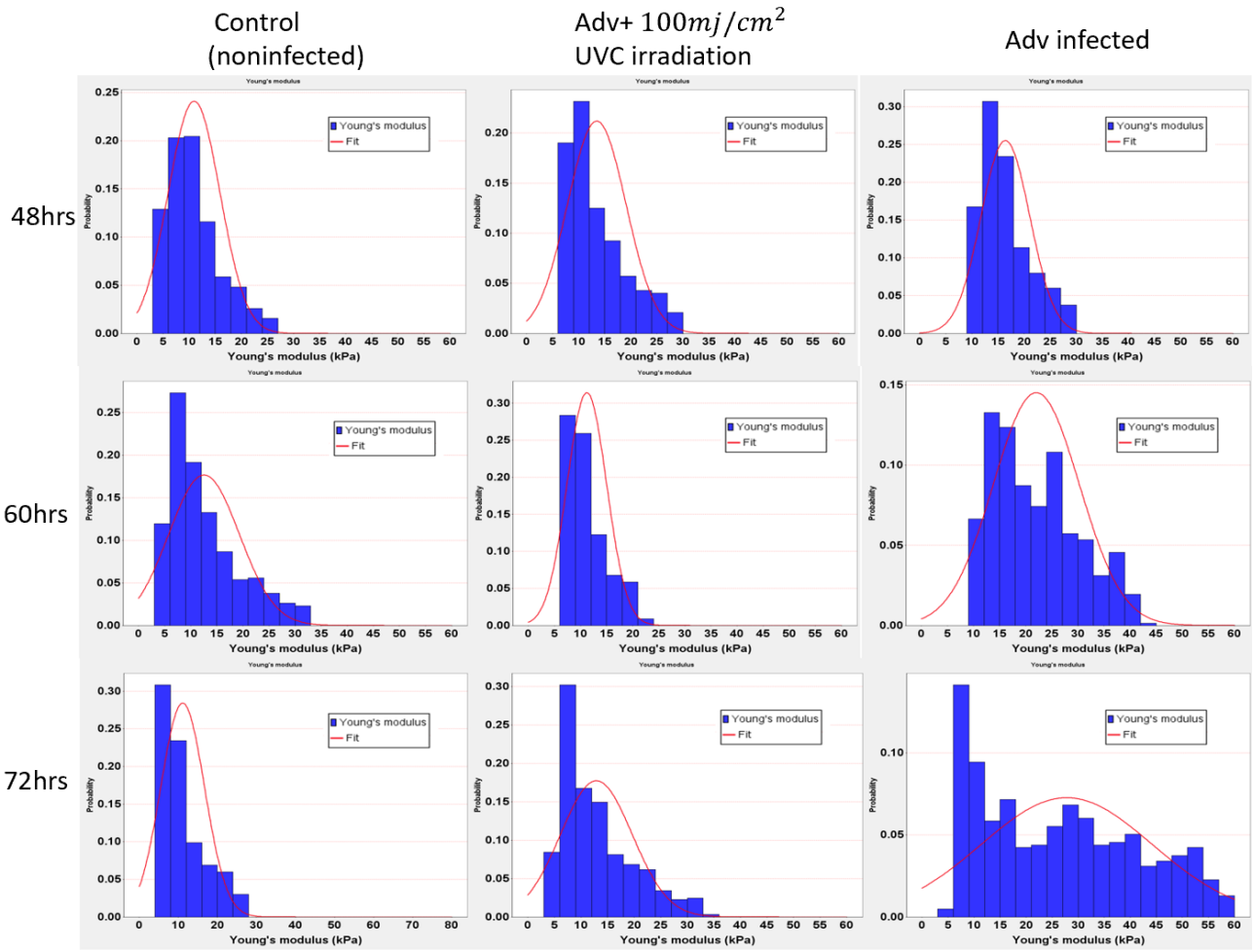

Fig. 9. The Young's Modulus distributions of cells on the central location for different groups: control; 100 UVC irradiation adenovirus infection; adenovirus injection from 48 to 72 hrs after virus starvation: Control: 10.94±4.96kPa, 12.53±6.77kPa, 11.10±5.61kPa; UVC disinfection: 13.46±4.54kPa, 11.20±3.80Kpa, 12.88±6.74Kpa; adenovirus: 16.40±4.68kPa, 22.03±8.24kPa, 27.79±16.47kPa, respectively. (Biological Repeat N> 3; 256 curves per cell; p< 0.01).

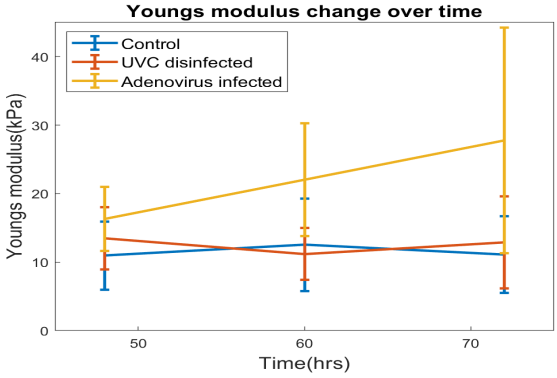

Fig. 10. Young's modulus of Vero E6 cells under different condition

permeability, cytoskeleton structure, cell-to-cell junction, and osmotic pressure are changed during the time lapse. Those organelle and inner liquid environment correlated to affect the stiffness of cells[38], [39].The mechanical properties of infected cells changed during the time lapse while the genome damaged virus would not affect the mechanical behavior of Vero E6 cells. With the cell continuously shrinking and rounding, the focal adhesion complex between the cell and substrate gradually loses its integrity, indicating the apoptosis of cells, however it is impossible for AFM to record this procedure once the cell loses binds to the substrate.

Overall, the viral genomes of viruses and bacteria are thoroughly disrupted with the 270nm UVC irradiation over very short time, which indicates the deep UVC LEDs as swift and clean approach to prevent further aggravation of this pandemic. With the established approach to evaluate UVGI disinfection effects, the single microorganism morphology and mechanical change could be measured without disrupting themselves, hence the disinfection effects could be assessed without time-consuming experiments such as in-use test of bacteria and immunofluorescence for virus evaluation. The proposed study could help the industry to design UVC-based disinfection tools with less human power consumption and more accuracy. Furthermore, to study living cell mechanical change with the tracking of single cells have brought us an understanding of how viruses gradually destroy the architecture of cellular integrity, which is one of the significant fields to further investigate into, helping pharmaceutical development and virus disinfector designs.

V. Conclusion

In this paper, to systematically study the 270nm deep UV irradiation disinfection effects on bio-organism, first the high power UVC LED array was designed and embedded into an automatic robot, with the high-resolution topography measured by AFM system and contrast fluorescence measurement and bacteria TSA test. With the increment of UVGI, the survival rate of E.coli decreases and the infectious ability of viruses reduces. Our findings also show outer capsid of adenovirus and the shell of E.coli still remain intact after a high dosage of deep UVGI irradiation, however the mechanical properties of E.coli have been changed which may cause by the damage of DNA strands or the protein functional groups which indicate the deep UVGI ability of selectively disrupt the strands of genome of bio-organism or the functional protein groups instead of the destruction of whole structure integrity.

The cell incubator system combining AFM was established to measure the real-time change of cellular morphology and mechanical change with the tracking of single cells. Compared with the control and 270nm UVGI-disinfected groups, the adenovirus-infected Vero cells suffer from dramatic morphology and stiffness change. The cell gradually separated from each other, and the focal adhesion complex was gradually disrupted and no longer possessed the ability of adhere to the substrate, which was cause by the shrinkage and disturbance of the focal adhesion complex. The findings contribute to a deeper understanding of cell behavior under an infectious situation and strengthen the effects of deep UVGI disinfection effects on viruses.

Acknowledgment

The authors would like to thank Mr. Siyu Wang and Dr. Qingyang Wang of department of industial and manufacturing systems engineering, the university of Hong Kong for the development of the UVC autonomous robot.

References

[1] S. Kooraki, M. Hosseiny, L. Myers, and A. Gholamrezanezhad, "Coronavirus (covid-19) outbreak: what the department of radiology should know," *Journal of the American college of radiology*, vol. 17, no. 4, pp. 447–451, 2020.

[2] R. Hirose, Y. Itoh, H. Ikegaya, H. Miyazaki, N. Watanabe, T. Yoshida, R. Bandou, T. Daidoji, and T. Nakaya, "Differences in environmental stability among sars-cov-2 variants of concern: Omicron has higher stability," *bioRxiv*, 2022.

[3] G. Kampf, D. Todt, S. Pfaender, and E. Steinmann, "Persistence of coronaviruses on inanimate surfaces and their inactivation with biocidal agents," *Journal of hospital infection*, vol. 104, no. 3, pp. 246–251, 2020.

[4] R. L. Hulkower, L. M. Casanova, W. A. Rutala, D. J. Weber, and M. D. Sobsey, "Inactivation of surrogate coronaviruses on hard surfaces by health care germicides," *American journal of infection control*, vol. 39, no. 5, pp. 401–407, 2011.

[5] H. Rabenau, G. Kampf, J. Cinatl, and H. W. Doerr, "Efficacy of various disinfectants against sars coronavirus," *Journal of Hospital Infection*, vol. 61, no. 2, pp. 107–111, 2005.

[6] G. Kampf, "Potential role of inanimate surfaces for the spread of coronaviruses and their inactivation with disinfectant agents," *Infection Prevention in Practice*, vol. 2, no. 2, p. 100044, 2020.

[7] M. Kneissl, T.-Y. Seong, J. Han, and H. Amano, "The emergence and prospects of deep-ultraviolet light-emitting diode technologies," *nature photonics*, vol. 13, no. 4, pp. 233–244, 2019.

[8] S. E. Beck, H. Ryu, L. A. Boczek, J. L. Cashdollar, K. M. Jeanis, J. S. Rosenblum, O. R. Lawal, and K. G. Linden, "Evaluating uv-c led disinfection performance and investigating potential dual-wavelength synergy," *Water research*, vol. 109, pp. 207–216, 2017.

[9] D. Battigelli, M. Sobsey, and D. Lobe, "The inactivation of hepatitis a virus and other model viruses by uv irradiation," *Water Science and Technology*, vol. 27, no. 3-4, pp. 339–342, 1993.

[10] A. C. Lai and S. S. Nunayon, "A new uvc-led system for disinfection of pathogens generated by toilet flushing," *Indoor air*, vol. 31, no. 2, pp. 324–334, 2021.

[11] M. Bormann, M. Alt, L. Schipper, L. van de Sand, M. Otte, T. L. Meister, U. Dittmer, O. Witzke, E. Steinmann, and A. Krawczyk, "Disinfection of sars-cov-2 contaminated surfaces of personal items with uvc-led disinfection boxes," *Viruses*, vol. 13, no. 4, p. 598, 2021.

[12] J. E. Jones, V. Le Sage, and S. S. Lakdawala, "Viral and host heterogeneity and their effects on the viral life cycle," *Nature Reviews Microbiology*, vol. 19, no. 4, pp. 272–282, 2021.

[13] K. Moriishi and Y. Matsuura, "Mechanisms of hepatitis c virus infection," *Antiviral Chemistry and Chemotherapy*, vol. 14, no. 6, pp. 285–297, 2003.

[14] M. Raeiszadeh and B. Adeli, "A critical review on ultraviolet disinfection systems against covid-19 outbreak: applicability, validation, and safety considerations," *Acs Photonics*, vol. 7, no. 11, pp. 2941–2951, 2020.

[15] G. Reybrouck, "The testing of disinfectants," *International biodeterioration & biodegradation*, vol. 41, no. 3-4, pp. 269–272, 1998.

[16] H. Rabenau, J. Cinatl, B. Morgenstern, G. Bauer, W. Preiser, and H. Doerr, "Stability and inactivation of sars coronavirus," *Medical microbiology and immunology*, vol. 194, no. 1, pp. 1–6, 2005.

[17] J. Herrera-Vásquez, M. Córdoba-Sellés, M. Cebrián, A. Alfaro-Fernández, and C. Jordá, "Seed transmission of melon necrotic spot virus and efficacy of seed-disinfection treatments," *Plant Pathology*, vol. 58, no. 3, pp. 436–442, 2009.

[18] A. Persat, C. D. Nadell, M. K. Kim, F. Ingremeau, A. Siryaporn, K. Drescher, N. S. Wingreen, B. L. Bassler, Z. Gitai, and H. A. Stone, "The mechanical world of bacteria," *Cell*, vol. 161, no. 5, pp. 988–997, 2015.

[19] P. L. Graumann, "Dynamics of bacterial cytoskeletal elements," *Cell motility and the cytoskeleton*, vol. 66, no. 11, pp. 909–914, 2009.

[20] H. G. Garcia, P. Grayson, L. Han, M. Inamdar, J. Kondev, P. C. Nelson, R. Phillips, J. Widom, and P. A. Wiggins, "Biological consequences of tightly bent dna: the other life of a macromolecular celebrity," *Biopolymers: Original Research on Biomolecules*, vol. 85, no. 2, pp. 115–130, 2007.

[21] A. Basu, D. G. Bobrovnikov, Z. Qureshi, T. Kayikcioglu, T. T. Ngo, A. Ranjan, S. Eustermann, B. Cieza, M. T. Morgan, M. Hejna, *et al.*, "Measuring dna mechanics on the genome scale," *Nature*, vol. 589, no. 7842, pp. 462–467, 2021.

[22] M. Li, N. Xi, Y. Wang, and L. Liu, "Atomic force microscopy in probing tumor physics for nanomedicine," *IEEE Transactions on Nanotechnology*, vol. 18, pp. 83–113, 2018.

[23] K. Xu, W. Sun, Y. Shao, F. Wei, X. Zhang, W. Wang, and P. Li, "Recent development of peakforce tapping mode atomic force microscopy and its applications on nanoscience," *Nanotechnology Reviews*, vol. 7, no. 6, pp. 605–621, 2018.

[24] Y. Yang, B. Zeng, Z. Sun, A. M. Esfahani, J. Hou, N.-D. Jiao, L. Liu, L. Chen, M. D. Basson, L. Dong, *et al.*, "Optimization of protein–protein interaction measurements for drug discovery using afm force spectroscopy," *IEEE transactions on nanotechnology*, vol. 18, pp. 509–517, 2019.

[25] C. A. Putman, K. O. Van der Werf, B. G. De Grooth, N. F. Van Hulst, and J. Greve, "Tapping mode atomic force microscopy in liquid," *Applied physics letters*, vol. 64, no. 18, pp. 2454–2456, 1994.

[26] D. J. Muller, "Afm: a nanotool in membrane biology," *Biochemistry*, vol. 47, no. 31, pp. 7986–7998, 2008.

[27] A. Stylianou, M. Lekka, and T. Stylianopoulos, "Afm assessing of nanomechanical fingerprints for cancer early diagnosis and classification: from single cell to tissue level," *Nanoscale*, vol. 10, no. 45, pp. 20 930–20 945, 2018.

[28] A. Ortega-Esteban, A. J. Pérez-Berná, R. Menéndez-Conejero, S. Flint, C. S. Martin, and P. J. de Pablo, "Monitoring dynamics of human adenovirus disassembly induced by mechanical fatigue," *Scientific reports*, vol. 3, no. 1, pp. 1–7, 2013.

[29] A. Ataei-Pirkooh, A. Alavi, M. Kianirad, K. Bagherzadeh, A. Ghasempour, O. Pourdakan, R. Adl, S. J. Kiani, M. Mirzaei, and B. Mehravi, "Destruction mechanisms of ozone over sars-cov-2," *Scientific reports*, vol. 11, no. 1, pp. 1–10, 2021.

[30] Y. Ma, N. Xi, Y. Xue, S. Wang, Q. Wang, and Y. Gu, "Development of a uvc-based disinfection robot," *Industrial Robot: the international journal of robotics research and application*, 2022.
[31] Y. Xue, M. Zhang, X. Liu, Y. Ma, and N. Xi, "Real-time tracking of living cell proliferation with nano mechanical biomarkers," in *2022 IEEE 17th International Conference on Nano/Micro Engineered and Molecular Systems (NEMS)*. IEEE, 2022, pp. 116–121.
[32] P. Hermanowicz, M. Sarna, K. Burda, and H. Gabryś, "Atomicj: an open source software for analysis of force curves," *Review of Scientific Instruments*, vol. 85, no. 6, p. 063703, 2014.
[33] G. R. Nemerow, P. L. Stewart, and V. S. Reddy, "Structure of human adenovirus," *Current opinion in virology*, vol. 2, no. 2, pp. 115–121, 2012.
[34] A. C. Marriott and N. Dimmock, "Defective interfering viruses and their potential as antiviral agents," *Reviews in medical virology*, vol. 20, no. 1, pp. 51–62, 2010.
[35] E. Matsuo, C. C. Celma, M. Boyce, C. Viarouge, C. Sailleau, E. Dubois, E. Bréard, R. Thiéry, S. Zientara, and P. Roy, "Generation of replication-defective virus-based vaccines that confer full protection in sheep against virulent bluetongue virus challenge," *Journal of virology*, vol. 85, no. 19, pp. 10 213–10 221, 2011.
[36] M. Biasin, A. Bianco, G. Pareschi, A. Cavalleri, C. Cavatorta, C. Fenizia, P. Galli, L. Lessio, M. Lualdi, E. Tombetti, *et al.*, "Uv-c irradiation is highly effective in inactivating sars-cov-2 replication," *Scientific Reports*, vol. 11, no. 1, pp. 1–7, 2021.
[37] S. Wang, H. Arellano-Santoyo, P. A. Combs, and J. W. Shaevitz, "Actin-like cytoskeleton filaments contribute to cell mechanics in bacteria," *Proceedings of the National Academy of Sciences*, vol. 107, no. 20, pp. 9182–9185, 2010.
[38] Q. Luo, D. Kuang, B. Zhang, and G. Song, "Cell stiffness determined by atomic force microscopy and its correlation with cell motility," *Biochimica et Biophysica Acta (BBA)-General Subjects*, vol. 1860, no. 9, pp. 1953–1960, 2016.
[39] S. Steltenkamp, C. Rommel, J. Wegener, and A. Janshoff, "Membrane stiffness of animal cells challenged by osmotic stress," *small*, vol. 2, no. 8-9, pp. 1016–1020, 2006.